Case Report

jfms OPEN REPORTS

Journal of Feline Medicine and Surgery Open Reports
1–9

DOI: 10.1177/20551169241303217
journals.sagepub.com/home/jfmsopenreports

This paper was handled and processed by the European Editorial Office (ISFM) for publication in *JFMS Open Reports*

Sage

Metastatic urothelial carcinoma in multiple appendicular muscles of a cat

Eduardo M Hernández[1], Pedro J Ginel[1], Beatriz Blanco[1], Yolanda Millán[2], Maria T Jiménez[3] and Elena Mozos[2]

Abstract

Case summary A 13-year-old male castrated domestic shorthair cat presented with a 2-month history of progressive lameness, poor appetite and constipation. Physical examination revealed palpable lesions in muscles of several extremities. Ultrasound examination confirmed the presence of round lesions with a hypo- or anechoic centre within the muscles. These lesions were characterised by an anechoic, occasionally trabeculated, central area surrounded by a hyperechoic band with heterogeneous echotexture. In total, seven lesions affecting six appendicular muscles were detected in different evolution stages, as suggested by their sizes and ultrasonographic features. Fine-needle aspiration of the muscle lesions revealed nests and isolated pleomorphic large neoplastic cells consistent with a carcinoma (vs sarcoma) and one mass was surgically removed. The histological and immunohistochemical studies confirmed a diagnosis of metastatic urothelial carcinoma. Although this neoplasia typically originates from the urothelium of the urinary bladder or renal pelvis, the primary tumour could not be detected in repeated abdominal ultrasound examinations. The cat was euthanased and further evaluations were declined by the author.

Relevance and novel information Urothelial carcinoma is a rare and highly aggressive neoplasia in the cat. While metastasis to regional lymph nodes and lungs are common in cats and dogs, to the authors' knowledge, there have been no reports of metastasis to multiple appendicular muscles in cats. This clinical presentation should be considered in the differential diagnoses of multiple nodular or cystic lesions affecting long muscles in cats.

Keywords: Urothelial carcinoma; appendicular muscles; muscle metastasis; muscle mass; ultrasonography, histopathology; immunohistochemistry

Accepted: 12 November 2024

Introduction

Urothelial carcinoma (UC), also known as transitional cell carcinoma, is a highly aggressive neoplasia in all species that is rare in cats.[1,2] In cats, the urinary bladder is the most common location of UC and less frequently may arise from the renal pelvis, ureters and urethra. The rate of metastases at the time of diagnosis is high, ranging from 12.7% to 20% of cases in cats with UC.[1,3] Metastases to lungs and lymph nodes are the most common but rare cases have been reported in other organs such as the large intestine, eye and abdominal wall.[1,3–5] This last location was mostly associated with needle tracts when cystocentesis was performed to biopsy the primary tumour.[6,7] A true muscle metastasis in one leg

[1]Department of Animal Medicine and Surgery, University of Córdoba, Campus de Rabanales, Córdoba, Spain
[2]Department of Anatomy, Comparative Pathology and Toxicology, University of Córdoba, Campus de Rabanales, Córdoba, Spain
[3]Mas Veterinaria, C\Arcos de la Frontera, Córdoba, Spain

Corresponding authors:
Eduardo M Hernández DVM, PhD, Department of Animal Medicine and Surgery, University of Córdoba, Campus de Rabanales, Córdoba, 14014, Spain
Email: pv2herom@uco.es

Pedro J Ginel DVM, PhD, Department of Animal Medicine and Surgery, University of Córdoba, Campus de Rabanales, Córdoba, 14014, Spain
Email: pginel@uco.es

was found incidentally during the necropsy of a cat with UC metastases to eyes and myocardium[5] but, to the best of the authors' knowledge, multiple metastases to appendicular long muscles have not been reported in cats with UC.

Case description

A castrated 13-year-old male domestic shorthair cat weighing 8 kg was presented to the institution with lameness, poor appetite and constipation, as well as progressive weight loss over the past 2 months. At the moment of presentation, renal parameters were indicative of an International Renal Interest Society (IRIS) stage 2. On palpation, several masses affecting the long muscles of the left forelimb and both hindlimbs were detected (Figure 1).

Radiographic examination of the affected limbs and thorax under sedation revealed an active periosteal reaction involving the cranial and medial proximal third of the left femoral diaphysis, changes in the shape of the right proximal fibula and increased radiopacity of the caudal thigh and caudal crural muscles related to the stifle (Figure 2). Thoracic radiographs showed a diffuse chronic interstitial pattern in the lungs.

Ultrasonography of the kidneys showed a bilaterally hyperechogenic renal cortex and irregular margins. The left kidney was smaller (3.51 × 2.93 cm) than the right kidney (4.63 × 2.49 cm), and both showed a hyperechoic wedge-shaped lesion, with the base at the renal capsule and apex at the corticomedullary junction, consistent with chronic renal infarction. No other significant changes were seen on ultrasonography of the lower urinary tract and abdomen (Figure 3).

A first ultrasound examination of the limbs (linear probe 10–12 MHz; Esaote Mylab 30 Gold VET; Probovet) revealed round to oval lesions characterised by an anechoic centre that contained more or less evident echogenic bands resembling a trabeculated structure, surrounded by a thick hyperechoic peripheral band (Figure 4a). All lesions were surrounded by muscle fibres but their size, as well as the muscles involved, varied among the affected limbs. The colour Doppler study of some of the lesions showed that they were poorly vascularised (grade 1)[8,9] (Figure 4b). In total, six different muscles presented lesions in three different limbs, and only the lateral head of the gastrocnemius muscle was bilaterally affected (Table 1). Initial treatment was symptomatic and consisted of robenacoxib 12 mg q24h 6 days (Onsior 6 mg; Elanco).

Figure 1 Left hindlimb skeletal muscle metastasis of an urothelial carcinoma before being surgically removed. The mass produced a deformity in the lateral head of the gastrocnemius muscle (circle)

The ultrasound examination was repeated 2 weeks later because of worsening clinical signs, including pain and difficulty standing to the point of ingesting food lying down. The size of the lesions was increased and the larger showed several anechoic centres with a peripheral band displaying hyperechoic areas with acoustic shadows (Figure 4c–f). An ultrasound-guided, fine-needle aspiration of a nodule from the lateral head of the right gastrocnemius muscle was performed and yielded a highly cellular sample with abundant large, pleomorphic tumour cells, isolated or forming cluster aggregates, admixed with cell debris (Figure 5a). Neoplastic cells displayed significant anisokaryosis and anisocytosis, large central or eccentric round nuclei, prominent nucleoli, and moderate to abundant basophil cytoplasm. Pale intracytoplasmic inclusions or vacuoles consistent with signet ring cells (Melamed-Wolinska bodies) were occasionally observed (Figure 5b). These findings were consistent with a malignant epithelial tumour and an excisional biopsy was recommended to achieve a definitive diagnosis. Under general anaesthesia, the lesion located within the lateral head of the left gastrocnemius muscle was completely excised.

Tissue samples were fixed in 10% neutral buffered formalin and embedded in paraffin wax. Sections, 4 µm in thickness, were stained with haematoxylin and eosin and Masson`s trichrome for morphological diagnosis. On the surgical section, the nodule showed a thick, firm and whitish wall delineating a narrow central cavity filled with necrotic cells debris (Figure 6a). Microscopically, the wall of the cystic nodule was formed by tubule-papillary structures covered by a neoplastic transitional epithelium (urothelium) supported by moderate to abundant fibrous stroma (Figure 6b,c). The outer layer of the epithelium showed characteristic round cells (umbrella cells) distinctive of urothelium. The cytoplasm was abundant with common eosinophilic and large pale acidophilic vacuoles consistent with Melamed-Wolinska bodies. Moreover, pseudocysts due to intraepithelial degeneration of neoplastic cells were often observed (Figure 6c). The mitotic

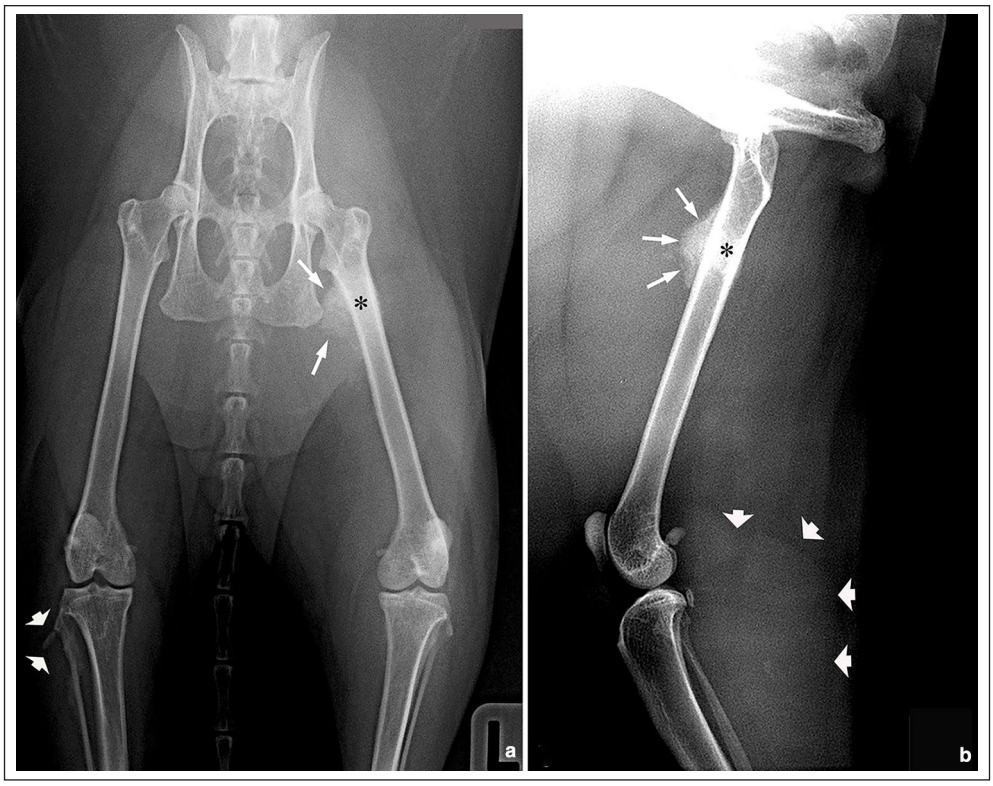

Figure 2 (a) Hip extended ventrodorsal radiographic projection including craneocaudal radiographic view of both stifles and (b) mediolateral projection of the left hip and stifle, at the time of presentation. There is a periosteal reaction, with less opacity than the bone, on the cranial and medial aspects of the femur (white arrows), as well as sclerosis in the corresponding area of the diaphysis (asterisks). The inner cortex or endosteum is intact. (a) There is also remodelling of the right proximal fibula (arrowheads), where a nodule was further detected by ultrasonography in the fibularis (peroneus) longus muscle. (b) In addition, increased radiopacity of soft tissue at the caudal aspect of the left stifle is present (arrowheads)

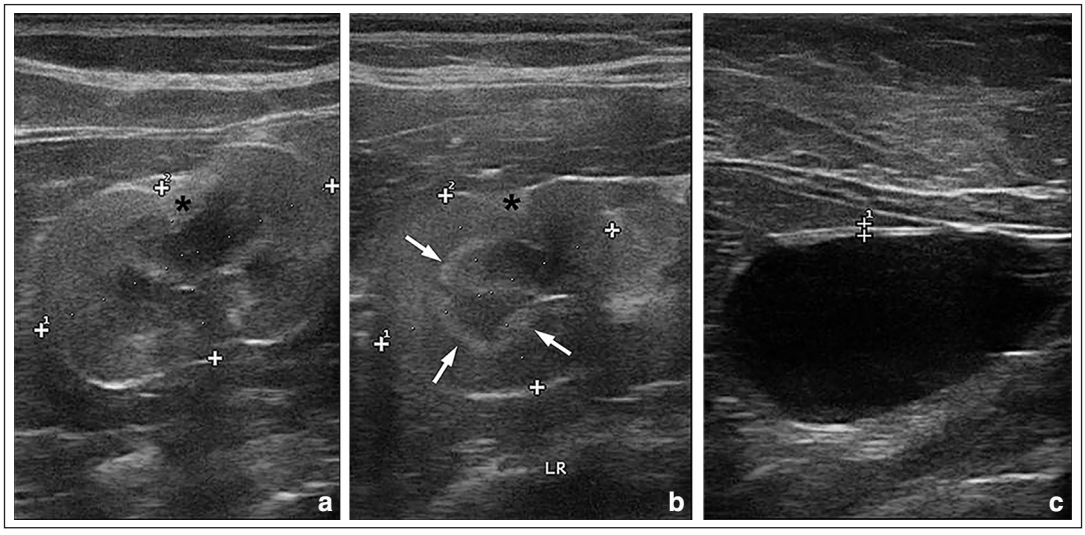

Figure 3 (a) Right kidney with normal size range, hyperechogenic cortex and irregular margins. A hyperechoic wedge-shaped section, consistent with chronic renal infarction, is seen in the renal cortex (asterisk). (b) The left kidney is slightly smaller than normal, also evidencing irregular margins, hyperechogenic cortex and an area of chronic renal infarction (asterisk); moreover, the caudal pole is structurally disorganised and a medullary band sign can be observed (arrows). (c) The ultrasonographic features of the urinary bladder are within normal limits

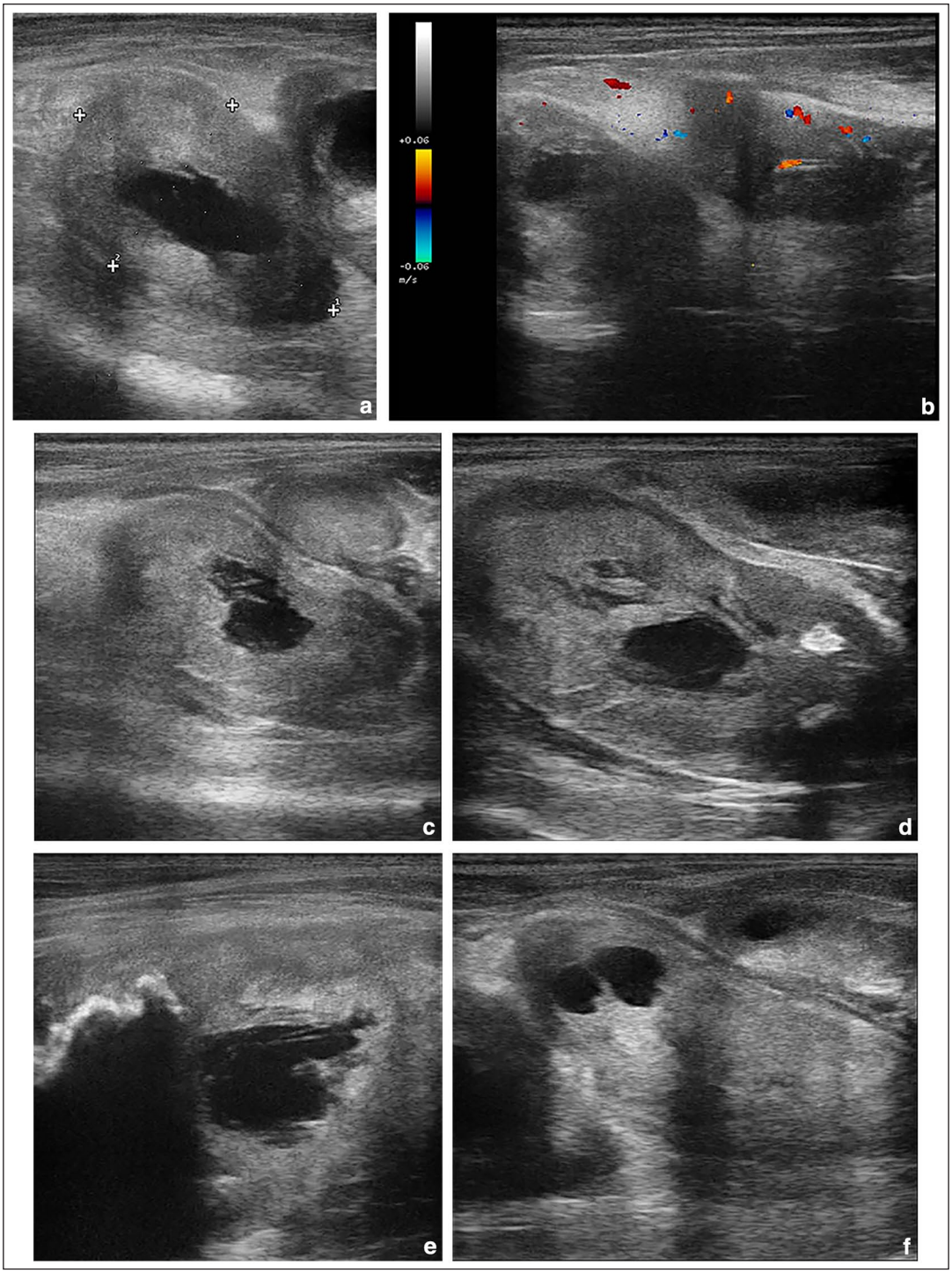

Figure 4 (a) Ultrasound images of the cystic mass located within the left semimembranous muscle. There is an anechoic central area with a band of hypoechoic organised tissue. (b) Colour Doppler visualisation of the lateral head of the left gastrocnemius muscle. Vascularisation of the mass is scarce (score 1) preferentially peripheral and occasionally central. (c) Longitudinal axis of the mass located in the superficial digital flexor muscle of the left hindlimb, as the lesions progressed the band of higher echogenicity was wider and more heterogeneous and the central anechoic area smaller sometimes with a trabeculated structure. (d) Superficial digital flexor muscle, the surrounding reactive tissue showed more hyperechogenic foci, with variable acoustic shadows, consistent with a higher degree of intralesional fibrosis. (e) Vastus medialis, there is periosteal reaction of the adjacent left femur proximal diaphysis. (f) Superficial digital flexor muscle, more advanced lesions showed anechoic foci located both in the central area and the surrounding connective band. The smallest nodule, located in the lateral head of the left gastrocnemius muscle, measured at the first visit 1.84 × 1.03 cm, whereas the largest recorded mass, measured 2 weeks later, affected the left superficial digital flexor muscle and had grown from 3.95 × 2.13 cm to a size of 5.36 × 2.63 cm

Table 1 Distribution and size of the urothelial carcinoma metastasis in the appendicular muscles at the first ultrasonography examination; the right forelimb was not affected

Left forelimb	Left hindlimb	Right hindlimb
Brachial triceps (long head) (3.19 × 1.76 cm)	Vastus medialis (4.43 × 2.67 cm) Semimembranosus (2.63 × 1.85 cm) Superficial digital flexor (3.95 × 2.13 cm) Gastrocnemius (lateral head) (1.84 × 1.03 cm)	Fibularis (peroneus) longus (3.74 × 3.70 cm) Gastrocnemius (lateral head) (3.44 × 2.06 cm)

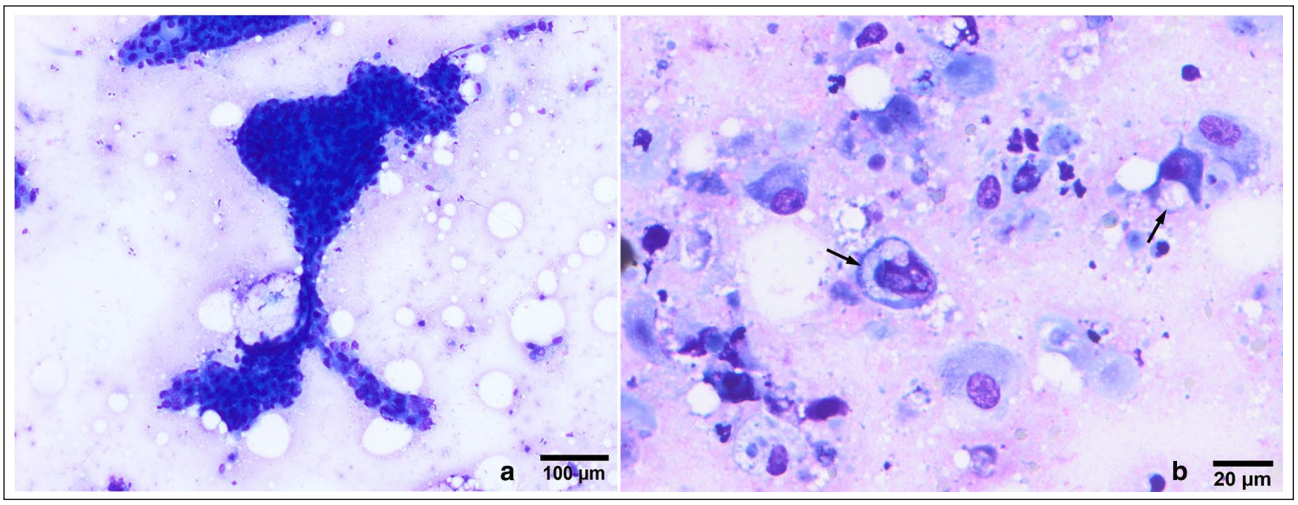

Figure 5 (a) Fine-needle aspiration cytology showing a large cluster of tumour cells. (b) Large, isolate and pleomorphic neoplastic cells between abundant cell debris, with occasional intracytoplasmic vacuoles (signet ring cells) (arrows) (Giemsa)

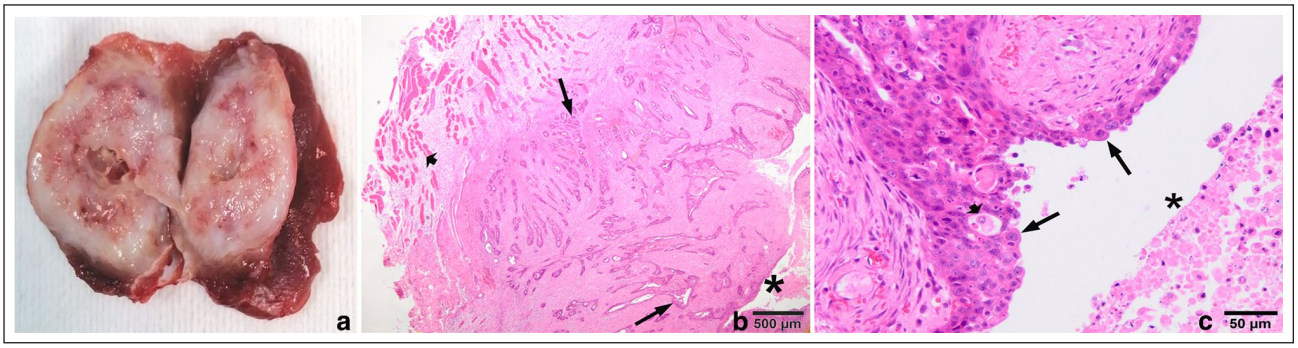

Figure 6 Gross and microscopic features of an intramuscular metastasis of a urothelial carcinoma. (a) Sagittal section of a well delimitated cystic-nodule showing a thick and whitish wall with a narrow lumen. (b) Microscopically, at low magnification, there are numerous infiltrating cords, nests and papillary structures of neoplastic urothelium (black arrows) conforming the tumour wall, which delineated a central lumen (see asterisks in [b] and [c]). Muscle fibres appear displaced at the outer part of the lesion (arrowhead). (c) Detail of the urothelium showing umbrella cells at the surface (black arrows), intracytoplasmic vacuoles (Melamed-Wolinska bodies) in intermediate layer and cystic degeneration of neoplastic cells (arrowhead)

count was high (>10 mitosis in an area of 2.37 mm^2). Overall, the histopathological features were consistent with a metastatic urothelial carcinoma exhibiting a cystic growth pattern.

An immunohistochemical study was performed to determine the phenotype of the tumour cells. The antibodies AE1–AE3 (pancytokeratin marker of epithelial cells), vimentin (marker of mesenchymal cells),

Table 2 Primary antibodies used in the immunohistochemical study

Antibody	Dilution	Antigen retrieval	Clone	Source
Cytoqueratin	1:100	10 mins protease 1%	AE1/AE3	Dako
Vimentin	1:100	10 mins protease 1%	Vim 3B4	Dako
Uroplakin III	1:20	15 mins citrate buffer pH 6.0 0.01 M 98°C	AU1	Progen
Cytokeratin 7	1:50	10 mins protease 1%	OV-TL 12/30	Dako
Cytokeratin 20	1:25	10 mins protease 1%	Ks.20.8	Dako
Ki67	1:75	40 mins citrate buffer pH 6.0 0.01 M 98°C	MIB-1	Agilent

uroplakin III (UPIII, specific membrane-protein marker of urothelial umbrella cells), cytokeratin (Ck)7 and Ck20 (markers of simple epithelium and urothelium), and Ki67 (marker of cellular proliferation) were evaluated using the avidin–biotin–peroxidase complex method (Table 2). Feline and canine urinary bladder was used as positive control. The proliferation index (PI) was evaluated quantitatively using 10 digital pictures of tissue sections taken at × 40 magnification from randomly selected neighbouring, non-overlapping fields. The number of positive and negative cells was counted with ImageJ, version 1.43 (National Institutes of Health). A minimum of 1000 tumour cells were counted and PI was expressed as the percentage of positive cells related to the total number of cells.

The neoplastic epithelial cells showed an intense and diffuse cytoplasmic immunolabelling for AE1/AE3 throughout all strata (Figure 7a). Vimentin antibody strongly reacted with the stroma of the tumour and rarely with neoplastic cells (Figure 7b). UPIII expression was weak–moderate–intense and randomly distributed throughout the neoplastic urothelium; individual superficial neoplastic cells, umbrella cells, strongly express UPIII (Figure 7c). CK7 antibody strongly reacted with many superficial cells but also was irregularly expressed by neoplastic cells of the intermedia and basal layers (Figure 7d). CK20 antibody showed weak and irregular immunolabelling of all layers of the neoplastic urothelium (Figure 7e). Ki67 antibody was strongly expressed in numerous nuclei of the tumour cells (Figure 7f). The Ki67 index was 70%. Overall, these results confirmed the urothelial nature of the neoplastic cells, as well as the high PI of the metastasis.

Once the histopathological diagnosis of metastatic UC was made, the owner declined the performance of advance imaging examinations and the cat was euthanased. Necropsy for further evaluations of the primary and metastatic tumours was also refused.

Discussion

To the best of the authors' knowledge, this is the first report of a metastatic UC affecting multiple appendicular muscles in a cat, as well as its ultrasound description. Although the primary tumour could not be identified, the microscopic features of the neoplastic urothelium were so characteristic that they supported a definitive diagnosis of metastatic urothelial carcinoma. Microscopically, neoplastic cells exhibit both large pale acidophilic cytoplasmic vacuoles known as Melamed-Wolinska bodies, and intraepithelial pseudocysts filled with necrotic debris, which are two distinctive features of urothelial neoplasia.[4,10]

UPIII is considered the most specific marker of mammalian urothelial tumours, but anaplastic and metastatic UCs often lack UPIII expression,[5,11,12] as has been observed in this case. CK7 is less specific but slightly more sensitive than UPIII for urothelial tumours and is considered the antibody of choice when a suspected urothelial tumour is negative for UPIII, especially in metastasis, as for the case reported here.[11,13] The loss of UPIII and CK7 in urothelial carcinomas suggests a lack of differentiation or epithelial–mesenchymal transition that facilitates the infiltration.[5,12] CK20 is a less specific and sensitive marker of UC because it is also expressed by non-urothelial tumours,[11,13,14] but the concurrent expression of CK7 and the irregular expression of UPIII observed in this metastatic carcinoma allows a diagnosis of UC.

The most common location of UC in cats is the urinary bladder but many of the affected cats do not present clinical signs associated with the lower urinary tract.[2,3] In the present case, ultrasonographic examination of the urinary bladder was normal and there were no clinical signs of lower urinary tract disease as could be expected if the ureters or the urethra were the primary tumour location, suggesting that its most likely origin was in the kidney. Renal ultrasonography findings indicated acquired chronic disease but were inconclusive regarding the presence of the primary tumour. This lack of sensitivity of the ultrasound examination in cases of UC has been reported previously.[4,5] In two cats with ultrasonographic changes of chronic kidney disease, renal UC was diagnosed post mortem.[4] Therefore, given the absence of lower tract signs and ultrasound findings, it is likely that the primary tumour was small in size and located in the kidney, although its finding, and the finding of other potential metastatic lesions, was prevented by the lack of post-mortem examination, which is a limitation of this case report.

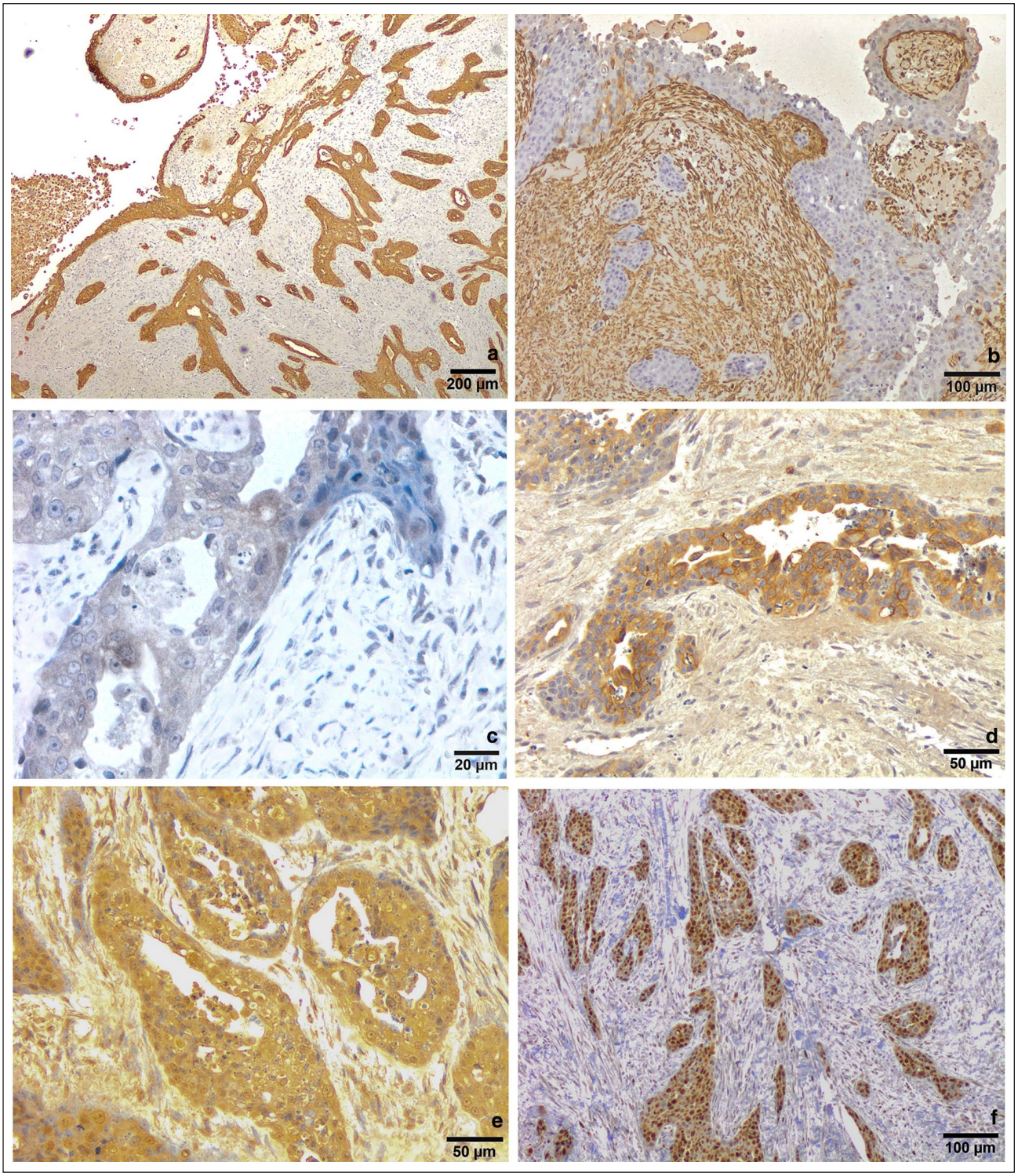

Figure 7 Intramuscular metastatic urothelial carcinoma. (a) AE1/AE3 antibody shows diffuse and strong labelling of all layers of the neoplastic urothelium. (b) Immunolabelling for vimentin is limited to the stroma of the nodule. The neoplastic urothelial cells are negative. (c) Uroplakin III expression is absent or weakly positive throughout the neoplastic urothelium, while many superficial neoplastic cells strongly react with the antibody. (d) Cytokeratin 7 expression is observed by numerous superficial umbrella cells and randomly reacted with isolated cells of the intermedia layers. (e) Cytokeratin 20 is moderately expressed throughout all cell layers. (f) Ki67 is strongly expressed by the nuclei of most tumour cells

In general, both primary and metastatic muscle tumours are rare in cats; reported prevalence in a retrospective study including 193 cats was 3.1% (ie, six cats). Carcinomas of different histological origin may result in musculoskeletal metastasis in the cat but, in a post-mortem study, UC had a prevalence of just 0.068%[10] and no previous reports have described the clinical signs and ultrasound features associated with them. The more common clinical signs in cats with muscle tumours, in descending order of prevalence, were anorexia, reluctance to move, depression, dyspnoea and lameness,[15] a clinical presentation in accordance with most of the clinical signs present in the case reported here.

Ultrasonography is highly sensitive for the diagnosis of muscle and tendon lesions,[16] but the ultrasonography features of musculoskeletal metastasis of UC have not been described. In this case, ultrasonography revealed a repetitive cystic pattern in all the metastases, which was correlated with the microscopic findings. The neoplastic urothelium grew to form a wall that delimited a lumen resembling the structure of the lower urinary tract. Apart from their cystic appearance, the metastases showed non-specific features common to most muscle tumours in cats, such as single lesions, round to oval shape and a mixed echogenic pattern, frequently with central hypo- or anechoic areas depending on the degree of necrosis.[15]

Conclusions

To the best of the authors' knowledge, this is the first report of multiple metastases to appendicular long muscles of a cat with UC. Although the primary tumour could not be located, the diagnosis was confirmed by histopathological and immunohistochemical analysis of the metastases. This unusual clinical presentation should be considered in the differential diagnoses of multiple nodular or cystic lesions affecting long muscles in cats.

Acknowledgements We thank the cat's owner for her understanding and willingness to help.

Conflict of interest The authors declared no potential conflicts of interest with respect to the research, authorship, and/or publication of this article.

Funding The article processing charge has been funded by research groups PAIDI BIO307 and AGR262, Junta de Andalucía, Spain.

Ethical approval The work described in this manuscript involved the use of non-experimental (owned or unowned) animals. Established internationally recognized high standards ('best practice') of veterinary clinical care for the individual patient were always followed and/or this work involved the use of cadavers. Ethical approval from a committee was therefore not specifically required for publication in *JFMS Open Reports*. Although not required, where ethical approval was still obtained, it is stated in the manuscript.

Informed consent Informed consent (verbal or written) was obtained from the owner or legal custodian of all animal(s) described in this work (experimental or non-experimental animals, including cadavers, tissues and samples) for all procedure(s) undertaken (prospective or retrospective studies). For any animals or people individually identifiable within this publication, informed consent (verbal or written) for their use in the publication was obtained from the people involved.

ORCID iD Pedro J Ginel https://orcid.org/0000-0002-9706-3715
Beatriz Blanco https://orcid.org/0000-0001-7056-3608
Elena Mozos https://orcid.org/0000-0003-0826-2171

References

1 Wilson HM, Chun R, Larson VS, et al. **Clinical signs, treatments, and outcome in cats with transitional cell carcinoma of the urinary bladder: 20 cases (1990–2004).** *J Am Vet Med Assoc* 2007; 231: 101–106.
2 Weyden L, O'Donnell M and Plog S. **Histological characterization of feline bladder urothelial carcinoma.** *J Comp Pathol* 2021; 182: 9–14.
3 Griffin MA, Culp WT, Giuffrida MA, et al. **Lower urinary transitional cell carcinoma in cats: clinical findings, treatments, and outcomes in 118 cases.** *J Vet Intern Med* 2020; 34: 274–282.
4 Hanzlicek A, Ganta C, Myers C, et al. **Renal transitional-cell carcinoma in two cats with chronic kidney disease.** *J Feline Med Surg* 2012; 14: 280–284.
5 Grader I, Southard TL and Neaderland MH. **Renal transitional cell carcinoma with bilateral ocular metastasis.** *JFMS Open Rep* 2016; 2. DOI: 10.1177/2055116916659516.
6 Nyland TG, Wallace ST and Wisner ER. **Needle-tract implantation following us-guided fine-needle aspiration biopsy of transitional cell carcinoma of the bladder, urethra, and prostate.** *Vet Radiol Ultrasound* 2002; 43: 50–53.
7 Higuchi T, Burcham GN, Childress MO, et al. **Characterization and treatment of transitional cell carcinoma of the abdominal wall in dogs: 24 cases (1985-2010).** *J Am Vet Med Assoc* 2013; 242: 499–506.
8 Öhberg L, Lorentzon R and Alfredson H. **Neovascularisation in Achilles tendons with painful tendinosis but not in normal tendons: an ultrasonographic investigation.** *Knee Surg Sports Traumatol Arthrosc* 2001; 9: 233–238.
9 Yeh C, Chen J, Li M, et al. **In vivo imaging of blood flow in the mouse Achilles tendon using high-frequency ultrasound.** *Ultrasonics* 2009; 49: 226–230.
10 Wimberly CK and Lewis RM. **Transitional cell carcinoma in the domestic cat.** *Vet Pathol* 1979; 16: 223–228.
11 Ramos-Vara JA, Miller MA, Boucher M, et al. **Immunohistochemical detection of uroplakin III, cytokeratin 7, and cytokeratin 20 in canine urothelial tumors.** *Vet Pathol* 2003; 40: 55–62.
12 Rasteiro AM, Lemos S, Oliveira PA, et al. **Molecular markers in urinary bladder cancer: applications for diagnosis, prognosis and therapy.** *Vet Sci* 2022; 9: 107. DOI: 10.3390/vetsci9030107.

13 Matsumoto K, Satoh T, Irie A, et al. **Loss expression of uroplakin III is associated with clinicopathologic features of aggressive bladder cancer.** *Urology* 2008; 72: 444–449.
14 Espinosa de los Monteros A, Fernández A, Millán MY, et al. **Coordinate expression of cytokeratins 7 and 20 in feline and canine carcinomas.** *Vet Pathol* 1999; 36: 179–190.
15 Vignoli M, Terragni R, Rossi F, et al. **Whole body computed tomographic characteristics of skeletal and cardiac muscular metastatic neoplasia in dogs and cats.** *Vet Radiol Ultrasound* 2013; 54: 223–230.
16 Kramer M, Gerwing M, Hach V, et al. **Sonography of the musculoskeletal system in dogs and cats.** *Vet Radiol Ultrasound* 1997; 38: 139–149.